

Direct Ion-Exchange Method for Preparing a Solution Allowing Spontaneous Perovskite Passivation via Hole Transport Material Deposition

Naoyuki Nishimura†, Hiroyuki Kanda†, Takurou N. Murakami†*

National Institute of Advanced Industrial Science and Technology (AIST), 1-1-1 Higashi, Tsukuba, Ibaraki 305-8565, Japan.

* Corresponding Author

Naoyuki Nishimura. E-mail: naoyuki-nishimura@aist.go.jp

1. Experimental methods

1-1. Materials

All materials were reagent grade and used as-purchased. 2-methoxyethanol and ethanol were purchased from WAKO-Chemicals Co. Ltd.. Formamidine hydroiodide (FAI), lead iodide (PbI₂), and *n*-octylammonium chloride (OACl) were purchased from Tokyo Chemical Industry Co. Ltd.. Methylammonium chloride (MACl) was purchased from Xian Polymer Co. Ltd. Mesoporous titanium oxide (m-TiO₂; 30NR) precursor was from Great Cell Solar. 2,2',7,7'-tetrakis-(*N,N*-di-4-methoxyphenylamino)-9,9'-spirobifluorene (Spiro-OMeTAD) was from Nippon Fine Chemical Co.. Other reagents were from Sigma Aldrich. Fluorine-doped tin oxide (FTO) coated transparent glass (thickness: 1.6 mm, sheet resistance $\leq 10 \Omega \text{ cm}^{-2}$) was purchased from Nippon Sheet Glass.

1-2. Preparation of HTM solution by the direct ion-exchange (DI) method

The DI method for preparation of HTM solution exhibiting spontaneous perovskite passivation function was carried out as follows: solid materials of 24 mM OACl, 24 mM Li-TFSI,¹ and 70 mM Spiro-OMeTAD were mixed into chlorobenzene (CB) and stirred for one hour at room-temperature, resulting in reddish-colored solution (Figure S2) containing Spiro-OMeTAD cation radical (Figure S3). Subsequently, the suspended solid was removed by filtration with 0.2 mm pored PTFE filter, and 15 $\mu\text{L mL}^{-1}$ of 4-*tert*-butylpyridine (TBP) was added into the filtrated solution.

1-2. *Synthesis of FAPbI₃ powder*

FAPbI₃ powder was synthesized as the precursor of the photoabsorber along with the previously reported method.²⁻⁴ 0.8 M of FAI and PbI₂ powders were dissolved into 2-methoxyethanol, and subsequently the solution was heated at 393 K for 1 h under continuous stirring. The black particles precipitated in the solution were immediately collected by filtration, and subsequently heated at 423 K for 30 min. Finally, the resultant black powder was further dried under evacuation at room temperature for 1 h.

1-3. *Solar cell fabrication*

The PSCs were prepared using the conventional methods with minor modifications.^{1, 3, 4} TiO₂ compact layer (~50 nm) were coated onto an FTO glass substrate, which was placed on a hotplate at 523 K, by spray pyrolysis using 4 vol% of titanium diisopropoxide bis(acetylacetae) ethanol solution. Subsequently, a m-TiO₂ layer was deposited by spin coating a mixture of 2-methoxyethanol (8424 μL), α-terpinol (158 μL), ethanol (4450 μL) and PST30NRD titanium oxide paste onto the substrate at 5000 rpm for 10 s, followed by heating the substrate at 773 K for 30 min.

FAPbI₃ perovskite layer was deposited onto the prepared TiO₂/FTO by spin coating in a dry room (temperature: 291 K, dew point: <243 K). 1.8 M of FAPbI₃ precursor solution was prepared by dissolving the synthesized FAPbI₃ powder (and 40 mol% for FAPbI₃ of MAI) into a mixture of *N,N*-dimethylformamide and dimethyl sulfoxide (4:1 vol ratio). The TiO₂/FTO substrate was spin-coated

with the prepared perovskite precursor solution at 6000 rpm for 50 s. During the spin coating, 500 μL of chlorobenzene (CB) was dropped after spinning for 10 s. The layer of the hole-transport material (HTM) was deposited by spin coating of the prepared solution via the DI method or a conventional method. The conventional HTM solution was prepared by dissolving 70 mM Spiro-OMeTAD, 0.27 mM TBP, followed by mixing the stock acetonitrile solutions of Li-TFSI and tris(2-(1H-pyrazol-1-yl)-4-*tert*-butylpyridine)-cobalt(III)tris(bis(trifluoromethylsulfonyl)imide (FK209) to be 35 mM and 4.2 mM, respectively. The prepared HTM solution were spin-coated at 3000 rpm for 30 s in the dry room. Finally, gold (Au) conductor layer with thickness of ~ 200 nm was deposited via thermal evaporation. The n-i-p structure PCSs were fabricated (Figure S1).

1-4. PV performance measurement

Current-voltage curves were measured using a source meter (R6243, ADVANTEST) and a class A solar simulator (XIL-05B100KP, Seric Co.) calibrated using an Si-reference cell equipped with a KG-5 filter to generate AM1.5G (100 mW cm^{-2}) at room temperature of ≈ 298 K in an ambient atmosphere. The current-voltage scan was performed under a constant speed of 100 mV s^{-1} under irradiation of the simulated sun light using a sample mask with an aperture area of 0.119 cm^2 . Before each measurement, an anti-reflection sheet was pasted onto the glass side of the cell. No pre-biasing was applied prior to the measurements. Over 30 samples were measured under each condition of the target and reference. Among the measured samples, the average PV parameters were calculated, and the best samples were

chosen. The stability test was conducted for more than 9 cells using environmental test chamber (Espec Co. Ltd.) for set at 30 °C (303 K) with relative humidity of 50% without sample encapsulation. The external quantum efficiency (EQE) action spectra were measured by with an action spectrum measurement setup (CEP-99W, Bunkou Keiki).

1-5. Characterizations

The UV-vis absorption spectra were measured with a spectrophotometer (UV3600, Shimazu). The PL lifetimes were measured using a time-correlated single photon counting system (Fluorolog-QM, Horiba) with an excitation at 665 nm. The PL lifetimes were estimated with double exponential fittings Origin© software. Ionization energies of HTMs were measured by photoelectron yield spectroscopy (PYS; BIP-KV100H, Bunkou Keiki). The wettability of the perovskite layer after removal of HTM layer ⁴ was assessed using a contact angle meter (Kyowa Interface Science Co.; DMo-401) The concentration of Li content in the HTM solution prepared by the DI method was estimated as follows: the HTM solution after the filtration was dried up at room temperature, and then washed with distilled water under stirring overnight. Subsequently, the resulting aqueous solution was filtrated by PTFE filter. Finally, the pH of the solution was adjusted to be an acid condition with distilled nitric acid, and then the solution was measured by inductively coupled plasma.

1. PSC structure

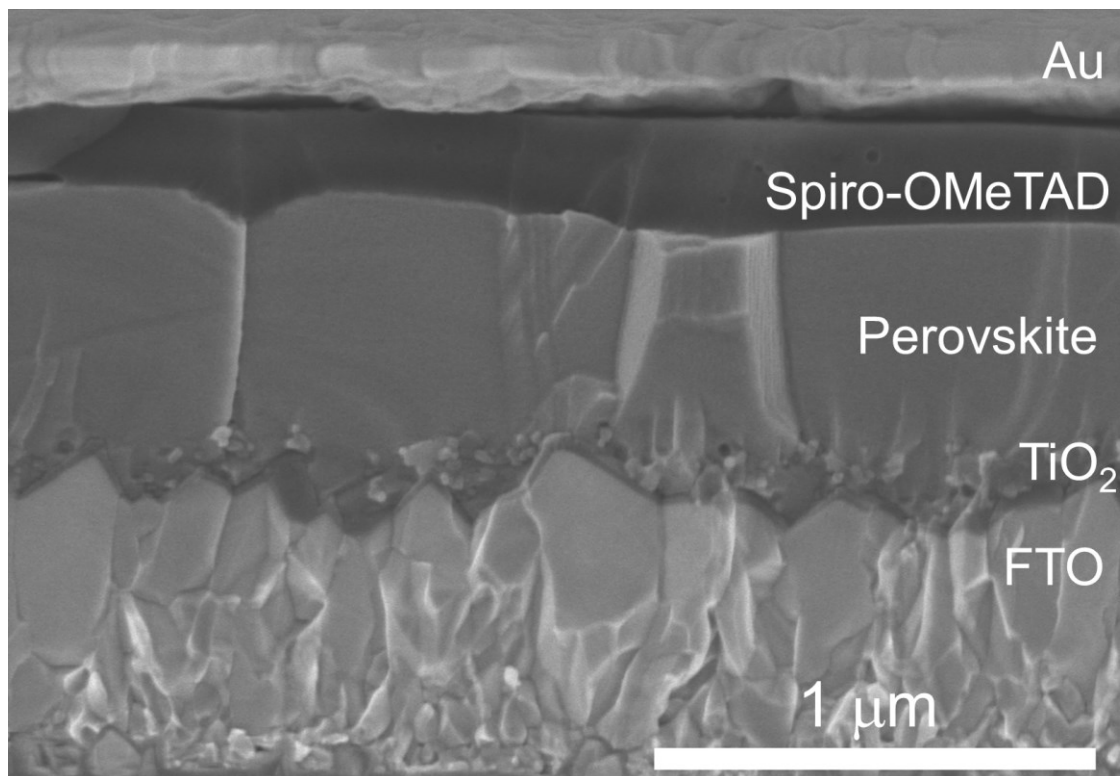


Figure S1. Cross sectional SEM image of the PSC using DI method

2. Spiro-OMeTAD radical formation in HTM solution prepared by DI method

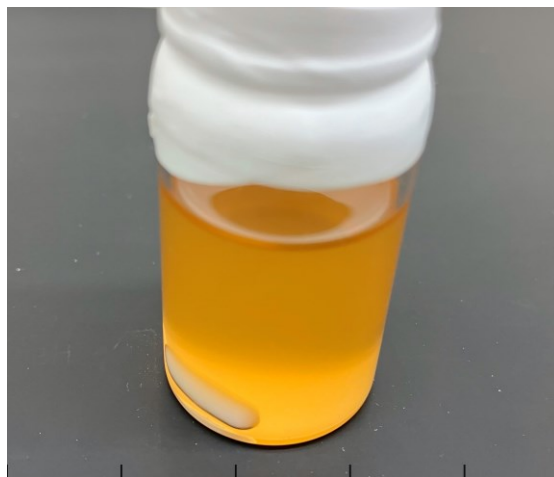


Figure S2. Picture of HTM solution prepared via DI method

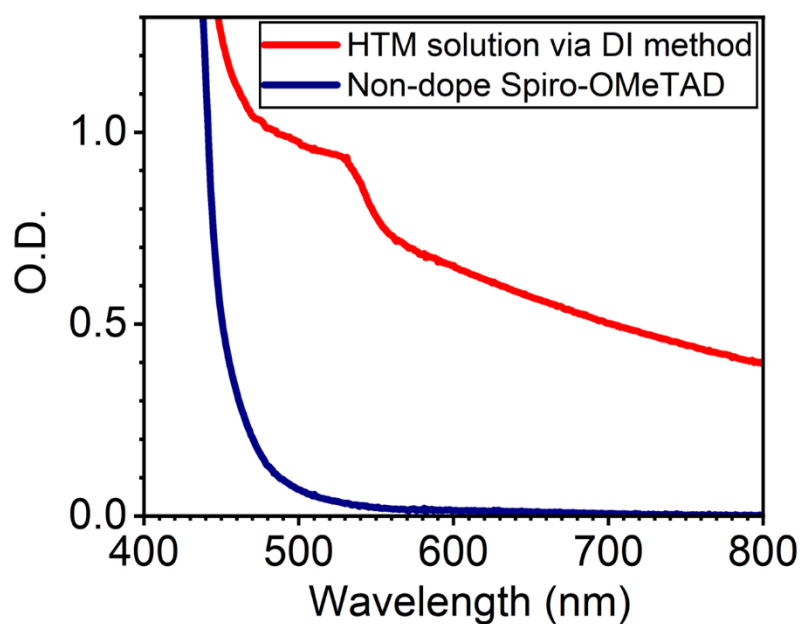


Figure S3. Absorption spectra of HTM solution via DI method and pristine Spiro-OMeTAD in CB; absorption peak at around 550 nm corresponding to Spiro-OMeTAD cationic radical^{1,5-9} was observed.

3. PV performances

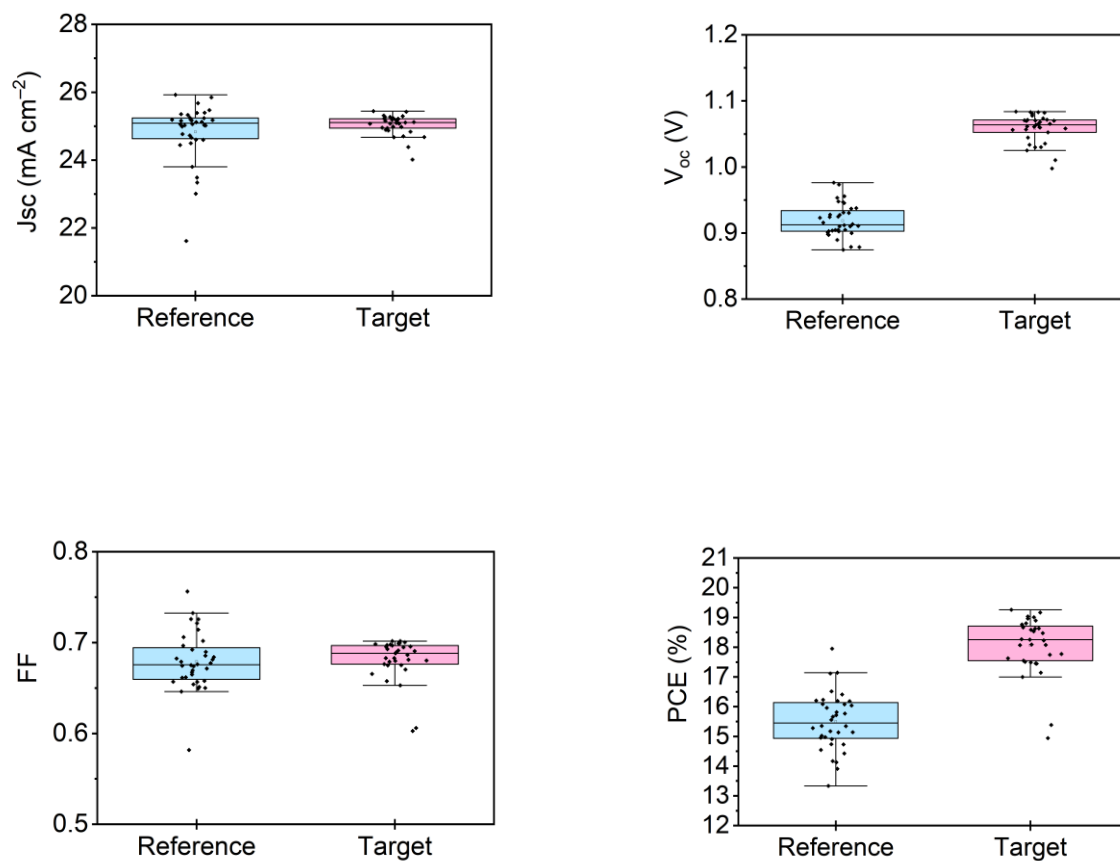


Figure S4. PV parameter distributions in forward scan

Table S1. Averages of PV parameters

Sample	Scan	J_{sc} (mA/cm^2)	V_{oc} (V)	FF	η (%)
Target	Backward	25.0 ± 0.3	1.11 ± 0.01	0.79 ± 0.02	21.8 ± 0.8
	Forward	25.0 ± 0.3	1.06 ± 0.02	0.68 ± 0.02	18.1 ± 1.0
Reference	Backward	24.8 ± 0.8	1.00 ± 0.02	0.78 ± 0.01	19.5 ± 0.8
	Forward	24.8 ± 0.8	0.92 ± 0.02	0.68 ± 0.03	15.5 ± 1.0

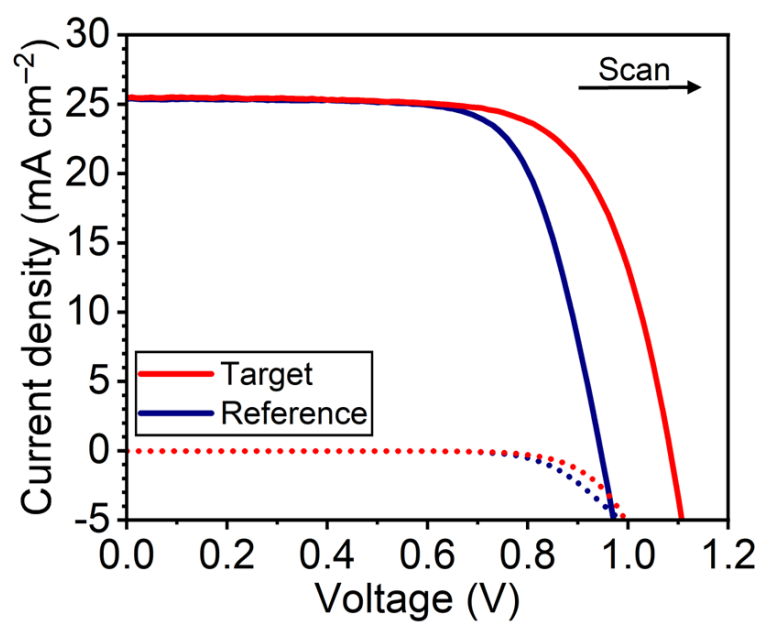


Figure S5. J-V curve of the best-performing PCSs in forward scan

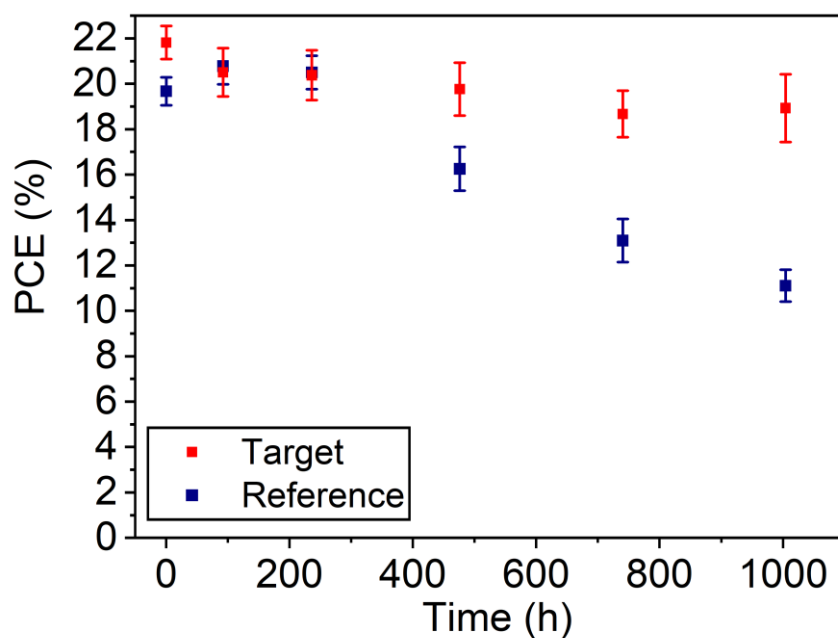


Figure S6. Long-term stability test (30°C, 50% relative humidity)

Reference

- (1) Nishimura, N.; Tachibana, H.; Katoh, R.; Kanda, H.; Murakami, T. N. Reactivity Manipulation of Ionic Liquid Based on Alkyl Primary Ammonium: Protonation Control Using Pyridine Additive for Effective Spontaneous Passivation of Perovskite via Hole Transport Material Deposition *ChemRxiv* **2024**, DOI: 10.26434/chemrxiv-2024-ts5k7
- (2) Jeong, J.; Kim, M.; Seo, J.; Lu, H.; Ahlawat, P.; Mishra, A.; Yang, Y.; Hope, M. A.; Eickemeyer, F. T.; Kim, M.; et al. Pseudo-halide Anion Engineering for Alpha-FAPbI₃ Perovskite Solar Cells. *Nature* **2021**, *592*, 381-385.
- (3) Nishimura, N.; Mathew, S.; Murakami, T. N. Suppressing Hydrogen Bonds and Controlling Surface Dipole: Effective Passivation for Hydrophobic Perovskite Photoabsorber Layers in Solar Cells. *New J. Chem.* **2023**, *47*, 4197-4201.
- (4) Nishimura, N.; Tachibana, H.; Katoh, R.; Kanda, H.; Murakami, T. N. Archetype-Cation-Based Room-Temperature Ionic Liquid: Aliphatic Primary Ammonium Bis(trifluoromethylsulfonyl)imide as a Highly Functional Additive for a Hole Transport Material in Perovskite Solar Cells. *ACS Appl. Mater. Interfaces* **2023**, *15*, 44859-44866.
- (5) Abate, A.; Hollman, D. J.; Teuscher, J.; Pathak, S.; Avolio, R.; D'Errico, G.; Vitiello, G.; Fantacci, S.; Snaith, H. J. Protic Ionic Liquids as p-dopant for Organic Hole Transporting Materials and Their Application in High Efficiency Hybrid Solar Cells. *J. Am. Chem. Soc.* **2013**, *135*, 13538-13548.
- (6) Geffroy, C.; Grana, E.; Bessho, T.; Almosni, S.; Tang, Z.; Sharma, A.; Kinoshita, T.; Awai, F.; Cloutet, E.; Toupance, T.; et al. p-Doping of a Hole Transport Material via a Poly(ionic liquid) for over 20% Efficiency and Hysteresis-Free Perovskite Solar Cells. *ACS Appl. Ener. Mater.* **2020**, *3*, 1393-1401.
- (7) Wang, S.; Yuan, W.; Meng, Y. S. Spectrum-Dependent Spiro-OMeTAD Oxidization Mechanism in Perovskite Solar Cells. *ACS Appl. Mater. Interfaces* **2015**, *7*, 24791-24798.
- (8) Schloemer, T. H.; Christians, J. A.; Luther, J. M.; Sellinger, A. Doping Strategies for Small Molecule Organic Hole-transport Materials: Impacts on Perovskite Solar Cell Performance and Stability. *Chem. Sci.* **2019**, *10*, 1904-1935.
- (9) Zhang, T.; Wang, F.; Kim, H. B.; Choi, I. W.; Wang, C.; Cho, E.; Konefal, R.; Puttison, Y.; Terado, K.; Kobera, L.; et al. Ion-Modulated Radical Doping of Spiro-OMeTAD for More Efficient and Stable Perovskite Solar Cells. *Science* **2022**, *377*, 495-501.